Progress In Electromagnetics Research Letters, Vol. 94, 57–65, 2020

Miniaturized Twelve-Stubbed Microstrip Balun with Twelfth Higher Order Harmonic Suppression and Improved Bandwidths

Vuppuloori Ravi Sekhara Reddy[1, *], Vamsi Krishna Velidi[2], and Bhima Prabhakara Rao[1]

Abstract—The design of a compact stubbed microstrip balun with very wide range higher order harmonic suppression is presented based on multiple open stub units, for which advantages are twofold, compared to single and double open-stub based designs. First, the high degree of size and harmonic reduction is achieved within the realizable impedance values. Second, the achieved bandwidths are fairly large (close to those of conventional balun) for a given set of electrical lengths. Unlike other methods, here, predetermined bandwidth analysis is provided for various levels of size and harmonic reduction. A prototype balun, having 75% size reduction and simultaneous wide higher order harmonic suppression extended up to $12f_0$, while maintaining good input matching, amplitude, and phase balance bandwidths, is fabricated for validation.

1. INTRODUCTION

Whenever it is intended to transform unbalanced single input signal into balanced differential signal, the foremost choice is a balun, which is a prominent microwave component. Baluns are crucial in a wide variety of applications like double balanced mixers, push pull amplifiers, frequency multipliers, and balanced antennas [1].

Several planar balun designs have been reported [2–11]. Marchand balun [2], using coupled lines, is difficult to realize and further requires compensation to match the even- and odd-mode phase velocities. The balun based on Wilkinson topology [3] requires a very large area and additional circuitry. In contrast, the branch-line balun (BLB) design [4–11], based on modified rat race coupler, entirely composed of transmission line sections, is simple and easy to implement, hence being the choice in wide attempts like dual-band operation [4, 5] and bandwidth enhancement [6, 7]. However, the circuit size of BLB is large due to the transmission line topology composed of half-wavelength lines; moreover, BLB exhibits harmonic responses, which interfere with other circuitries in system level. Addressing this, several methods were proposed in [8–11]. Transmission line equivalent shunt open-stub units with single and two stubs were presented in [8–10] for simultaneous size and harmonic reduction, while an inter digital capacitor like structure (resembling two stub unit) is presented in [11] only for miniaturization. However, the total size of the balun is large in [8] as the stubs were placed outside, while the amplitude imbalance is huge (0.9 dB) at operating frequency in [11]. Though a good size reduction was achieved in [9–11], the harmonic suppression was not wide, limited up to fourth [9] and sixth [10]. These were achieved at the expense of reduced balun bandwidths, which were not addressed in [8–11].

In this work, a multiple stub unit composed of three open-stubs (inverted E-shape) is proposed to obtain improved bandwidths compared to those obtained using single and two stubs [9, 10]. Here, special attention is paid to the prediction of several balun bandwidths such as input matching, amplitude, and phase balances, where the variation is examined for different line lengths, using detailed design graphs

Received 3 August 2020, Accepted 14 October 2020, Scheduled 24 October 2020

* Corresponding author: Vuppuloori Ravi Sekhara Reddy (ravisekharreddy.4@gmail.com).

[1] Department of ECE, Jawaharlal Nehru Technological University (JNTU), Kakinada, India. [2] Communication Systems Group, U. R. Rao Satellite Centre, Indian Space Research Organization (ISRO), India.

and tables. Furthermore, the present unit offers high degree of size reduction and harmonic suppression within the realizable impedance values compared to [8–10]. A prototype balun having 75% size reduction with a very wide range (up to twelfth) harmonic suppression is fabricated at 0.5 GHz for demonstration. The achieved bandwidths are better than [8–11], and the harmonic suppression range is double of [10].

2. DESIGN AND ANALYSIS

A multiple shunt open-stub unit, equivalent to a conventional quarter wavelength line, is shown in Fig. 1, where the cases with single stub [9], double stub [10], and the present triple stub units having T, II, and InvE-shapes, respectively, are highlighted. The present InvE-unit with three shunt open-stubs (Z_S, θ_S) and two connecting lines (Z_t, θ_t), shown in Fig. 2, is used to replace the quarter wavelength lines of the conventional balun and thus forming the present compact balun with twelve open-stubs. It is noted that the middle stub of the present InvE-shape unit is $Z_s/2$, and the implemented BLB will have twelve stubs with impedance $Z_s/2$ due to the parallel combination of two consecutive stubs of the six cascaded units.

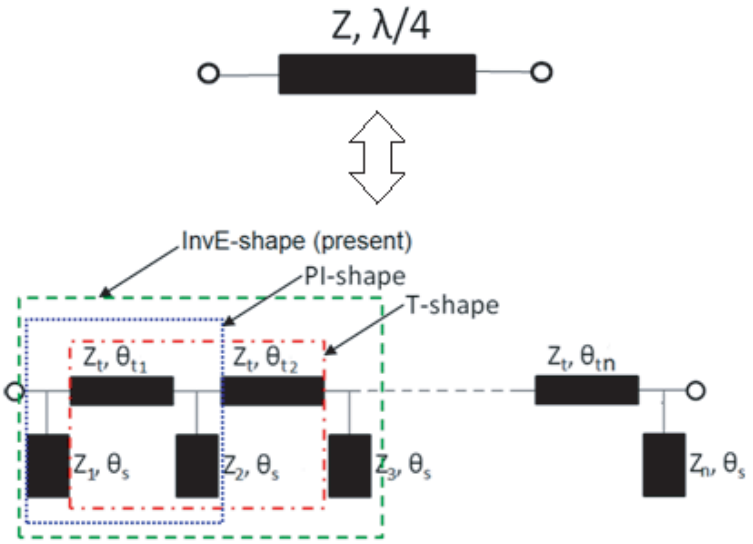

Figure 1. Traditional quarter-wavelength transmission line and its equivalent multiple-stub unit.

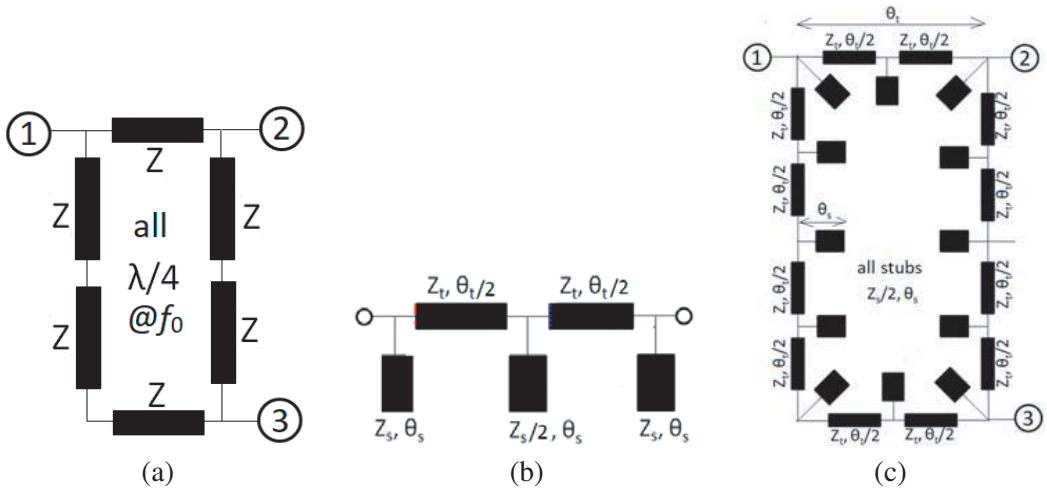

Figure 2. Transmission line topology of (a) conventional branch-line balun and (b) the proposed compact stubbed balun using three-stub InvE-units.

The choice of electrical lengths for the series arm and shunt-stub leads to miniaturization and harmonic suppression, respectively. The size reduction (M) and number of harmonics suppressed (N) are given in terms of electrical lengths [10] as

$$\begin{aligned} M &= 100\left[1-(\theta_t/90)^2\right] \quad \text{and} \\ N &= 2\left[floor\left(90/\theta_s\right)-1\right] \end{aligned} \tag{1}$$

From Eq. (1), higher orders for M and N are achieved for smaller values of θ_t and θ_s, respectively. However, the selection of electrical lengths is limited by the corresponding impedances of the lines. For a conventional quarter wavelength transmission line (QWTL), the $ABCD$ matrix is:

$$\begin{bmatrix} A & B \\ C & D \end{bmatrix}_{QWTL} = \begin{bmatrix} 0 & jZ \\ \dfrac{j}{Z} & 0 \end{bmatrix} \tag{2a}$$

The $ABCD$ matrix of the InvE-shape unit is obtained by multiplying the individual units of two series arms and three shunt open stub units.

$$\begin{aligned} \begin{bmatrix} A & B \\ C & D \end{bmatrix}_{InvE} = &\begin{bmatrix} 1 & 0 \\ \dfrac{j}{Z_S}\tan\theta_S & 1 \end{bmatrix} \times \begin{bmatrix} \cos(\theta_t/2) & jZ_t\sin(\theta_t/2) \\ \dfrac{j}{Z_t}\sin(\theta_t/2) & \cos(\theta_t/2) \end{bmatrix} \times \begin{bmatrix} 1 & 0 \\ \dfrac{2j}{Z_S}\tan\theta_S & 1 \end{bmatrix} \\ &\times \begin{bmatrix} \cos(\theta_t/2) & jZ_t\sin(\theta_t/2) \\ \dfrac{j}{Z_t}\sin(\theta_t/2) & \cos(\theta_t/2) \end{bmatrix} \times \begin{bmatrix} 1 & 0 \\ \dfrac{j}{Z_S}\tan\theta_S & 1 \end{bmatrix} \end{aligned} \tag{2b}$$

From Eq. (2b), $A_{InvE} = \cos\theta_t - 4\frac{Z_t}{Z_S}\sin(\theta_t/2)\cos(\theta_t/2)\tan\theta_S + 2(\frac{Z_t}{Z_S})^2\sin^2(\theta_t/2)\tan^2\theta_S$ and

$$B_{InvE} = 2Z_t\cos(\theta_t/2)\sin(\theta_t/2) - 2\left(\frac{Z_t}{Z_S}\right)^2\sin^2(\theta_t/2)\tan\theta_S \tag{2c}$$

The final impedances of the InvE-shape unit are obtained by equating Eqs. (2a) and (2c), and by solving

$$\begin{aligned} Z_t &= \frac{Z}{\sqrt{2}}\csc(\theta_t/2) \quad \textit{and} \\ Z_s &= \frac{Z\tan\theta_s}{\sqrt{2}\cos(\theta_t/2)-1} \end{aligned} \tag{2d}$$

Using Eqs. (1) and (2d), circuit computations of BLB are performed for different levels of size reduction and harmonic suppression responses. In each case, various fractional bandwidths (FBWs) are calculated and plotted to show the variation with θ_t and θ_s in Figs. 3 and 4, respectively. Here, first the FBWs of the conventional BLB are calculated and shown as solid lines. For comparison, the corresponding FBWs of the BLBs implemented using single and two-stub units of [9] and [10], respectively, are also plotted. Considering port 1 as the input port, the bandwidth criteria are defined as

$$\begin{aligned} |S_{11}| &: -20\,\text{dB}, \\ Mag.\,Bal.\,(|S_{31}| \sim |S_{21}|) &: 0 \pm 1.0\,\text{dB} \quad \text{and} \\ Phase\,Bal.\,(\angle S_{31} \sim \angle S_{21}) &: 180^\circ \pm 10^\circ \end{aligned} \tag{3}$$

To show the effect of miniaturization, the variations of FBWs of return loss, magnitude, and phase balances in Eq. (3), with θ_t for fixed θ_S (15° and 30°), are shown in Fig. 3. It can be observed that the FBWs decrease with reducing θ_t in all cases, but are closer to conventional BLB for the present three stub unit. Among the three cases in Eq. (3), the input matching is found to be greatly affected with miniaturization than the amplitude and phase balances. For instant comparison, the FBWs and the impedance values for BLB realization are compared in Table 1. For greater size reduction of $M = 75\%$ ($\theta_t = 45^\circ$), the input matching bandwidth is 32% for the present Inv-E shaped unit, while it is 21 and 22% for the single and two stub units, respectively. Hence the matching FBW is improved by about

10% in the present case. Similarly, an improvement of 4% and 2% is seen in the case of phase and magnitude balance bandwidths, respectively. However, the T-shaped unit is not suitable to achieve this level of size reduction as the impedance value (170 Ω) is beyond the realizable range, hence, the two-stub and three stub units are the possible solutions.

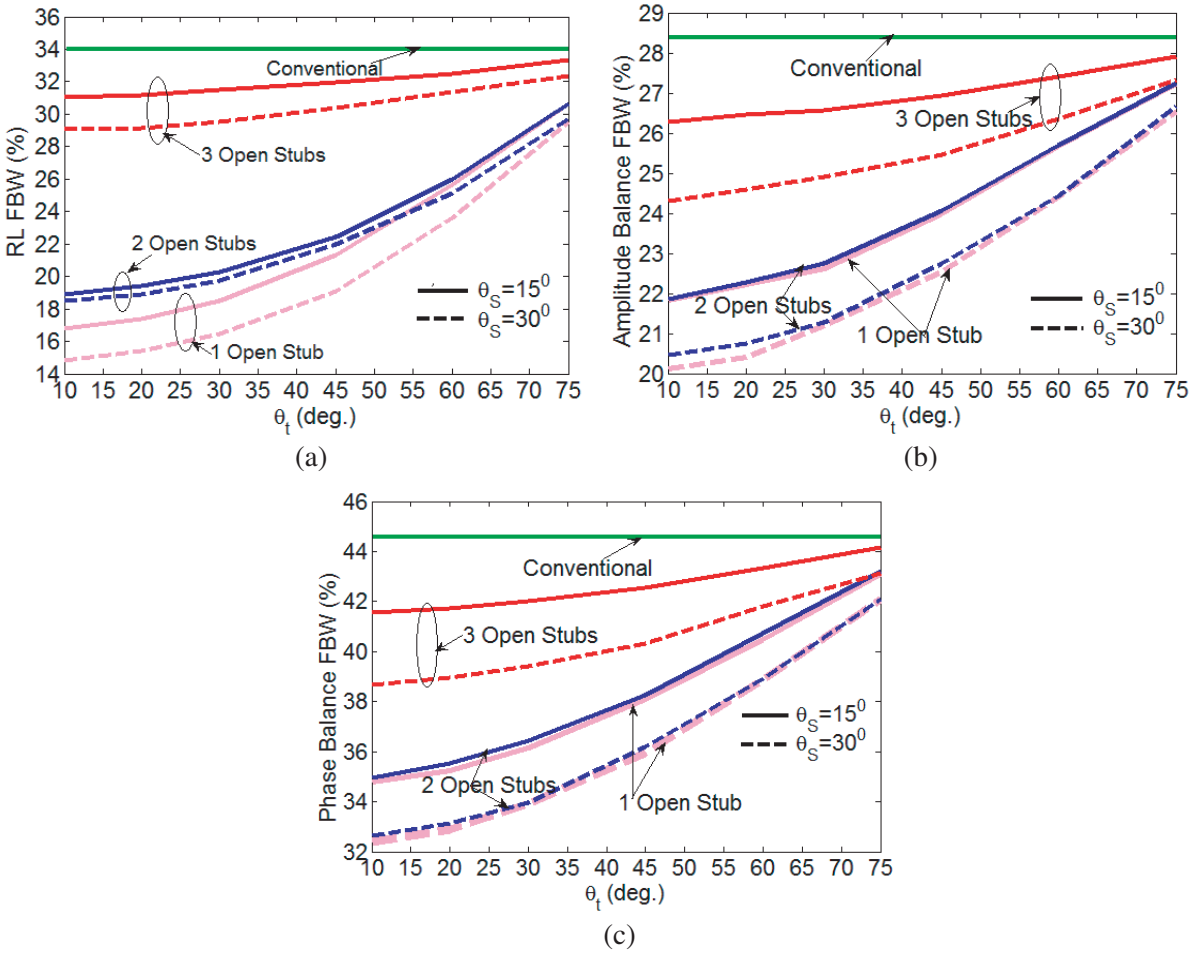

Figure 3. Variation of balun FBWs with miniaturization (θ_t) using single, double and three stub units. (a) Return loss, (b) magnitude balance and (c) phase balance.

Table 1. Line impedances and FBWs for T, Π and present Inv-E shaped units equivalent to $Z = 70.7\,\Omega$ For $N = 10$ ($\theta_s = 15°$) for various θ_t.

Parameter	**M = 55.6% (θ_t= 60°)**			**M = 25 % (θ_t = 45°)**		
	T [9]	**Π [10]**	**Present InvE**	**T [9]**	**Π [10]**	**Present InvE**
FBWs (%)						
RL (20 dB)	25.6	25.8	32.5	21.3	22.5	32.0
Phase bal. ($180° \pm 10°$)	40.5	40.7	43.4	38.0	38.2	42.6
Amp. bal. (0 ± 1 dB)	25.7	25.6	27.4	24.0	24.1	26.9
Impedances						
$Z_t(\Omega)$	122.5	81.6	100	170.7	100	130.6
$Z_S(\Omega)$	28.4	18.9	42.1	22.9	13.4	30.9

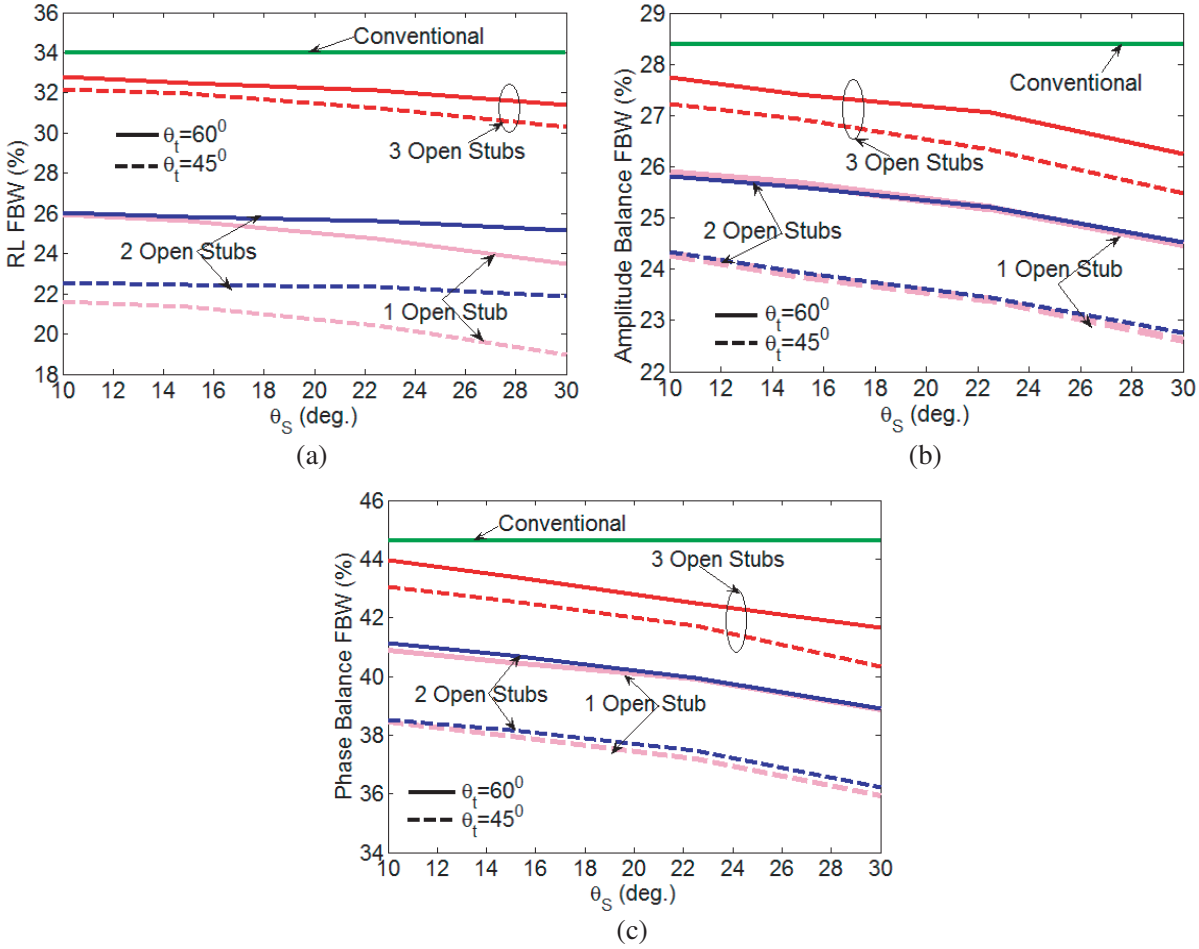

Figure 4. Variation of balun FBWs with harmonic suppression (θ_S) using single, double and three open-stub units. (a) Input matching. (b) Magnitude balance. (c) Phase balance.

Table 2. Line impedances and FBWs for T, Π and present Inv-E units for $M = 25\%$ ($\theta_t = 45$) for various θ_S.

Parameter	**N = 4 ($\theta_S = 30°$)**		**N = 10 ($\theta_S = 15°$)**	
	Π	**Present InvE**	**Π**	**Present InvE**
FBWs (%)				
RL (20 dB)	22.0	30.4	22.5	32.0
Phase bal. ($180° \pm 10°$)	36.2	40.3	38.2	42.6
Amp. bal. (0 ± 1 dB)	22.8	25.5	24.1	26.9
Impedances				
$Z_t(\Omega)$	100	130.6	100	130.6
$Z_S/2(\Omega)$	28.9	66.6	13.4	30.9

Similarly, the variations of FWBs, with stub length θ_S for fixed $M = 44.4\%$ and 25% ($\theta_t = 60°$ and $45°$), are shown for all cases of Eq. (3) in Fig. 4 for the single, two and present three stub units. Here, FBWs increase with decreasing θ_S; however, the variation is relatively minimal, compared to Fig. 3. For instance, the FBWs and impedances are compared in Table 2 for $\theta_S = 30°$ and $15°$ for fixed $\theta_t = 45°$. As discussed previously for the realizable impedance value, the single stub case is not shown here. From

$\theta_S = 30^\circ$ to 15°, the harmonic suppression is enhanced by two times (from six to twelve) with an overall improvement in FBWs by at least 2%. However, this case with $\theta_S = 15^\circ$ is difficult to implement using two stub units as the impedance required is too low (13.4 Ω), which results in stub placement problems. In contrast, the impedance required is approximately 31 Ω in the case of the present three stub unit that can be easily accommodated inside the ring geometry.

From the above discussions, it can be clearly highlighted that an improvement in FBW is obtained by choosing higher number of stubs having smaller stub lengths. Thus, triple stub unit is a fine choice in terms of improved FBW, miniaturization, and harmonic suppression compared to those in [9, 10].

3. FABRICATION AND MEASUREMENT

A low cost FR4 substrate having a dielectric constant of $\varepsilon_r = 4.3$, loss tangent 0.022, and thickness 1.58 mm was used to fabricate microstrip balun using present InvE-shaped unit at $f_0 = 0.5$ GHz. From Eq. (2d), the line impedance (Z_t) and stub impedance (Z_S) of each triple stub unit, corresponding to $Z = 70.7\,\Omega$, $\theta_t = 45^\circ$, and $\theta_S = 15^\circ$, are 130.6 Ω and 30.9 Ω, respectively.

EM simulations of the present balun were carried out using the Ansys HFSS full wave simulator. A photograph of the fabricated miniaturized balun is shown in Fig. 5 occupying an area of 47 mm × 94 mm, which is only 26% area of a conventional balun area (91 mm × 183 mm) at f_0.

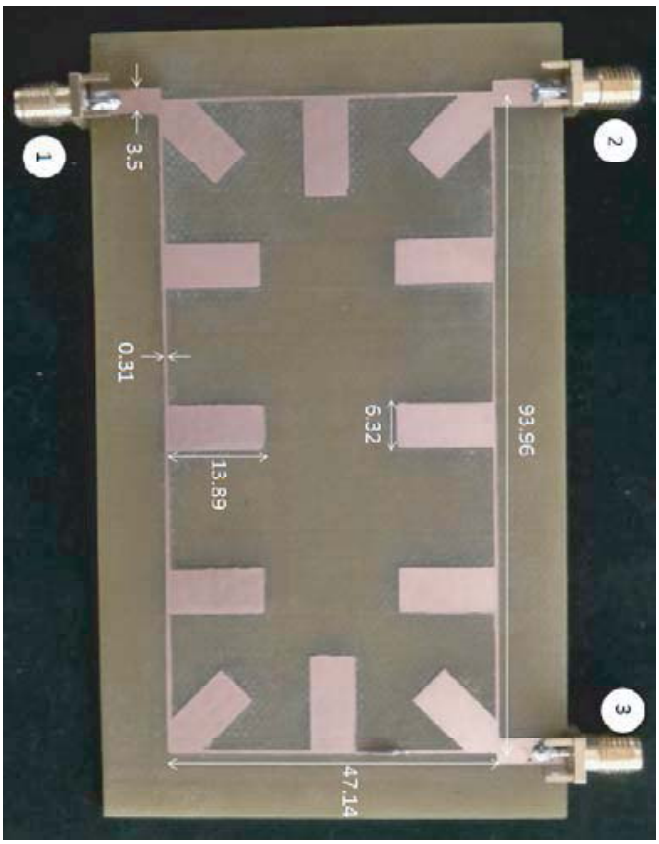

Figure 5. Photograph of the fabricated balun with dimensions (mm).

Measured, EM simulated, and circuit predicted magnitude responses, in Fig. 6, show good agreement. The measured insertions losses (including connector losses) S_{21} and S_{31} are 3.64 dB and 3.6 dB, respectively. The return loss is 15.7 dB at f_0 and 15 dB FBW 74%. The phase and amplitude balance responses are shown in Fig. 7. The measured phase difference and magnitude balance FBWs are 57% and 26%, respectively. Moreover, the proposed balun has no spurious response up to 6 GHz,

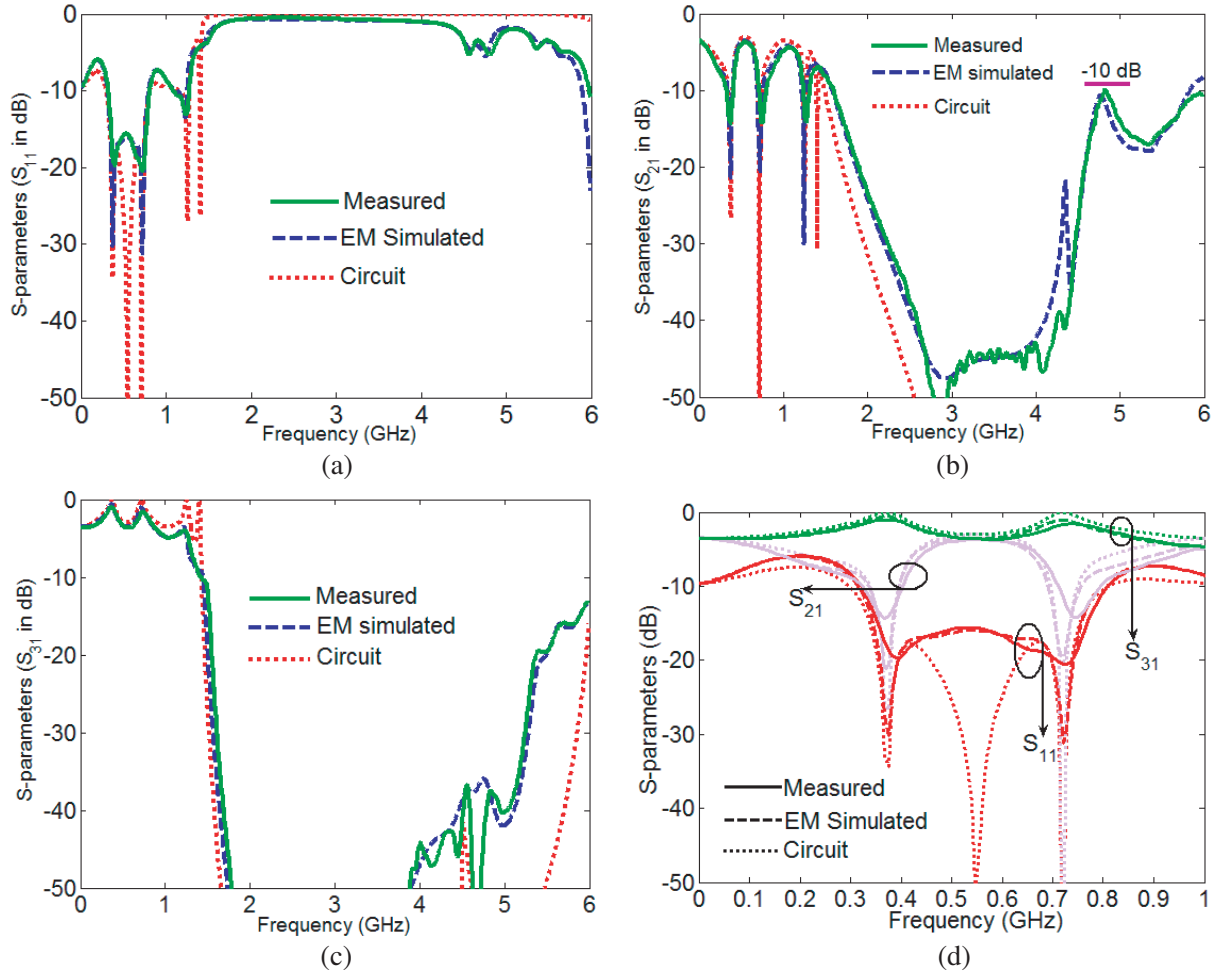

Figure 6. Measured, EM simulated, computed S-parameters. (a) S_{11}. (b) S_{21}. (c) S_{31}. (d) In band of proposed compact balun with wide range spurious suppression.

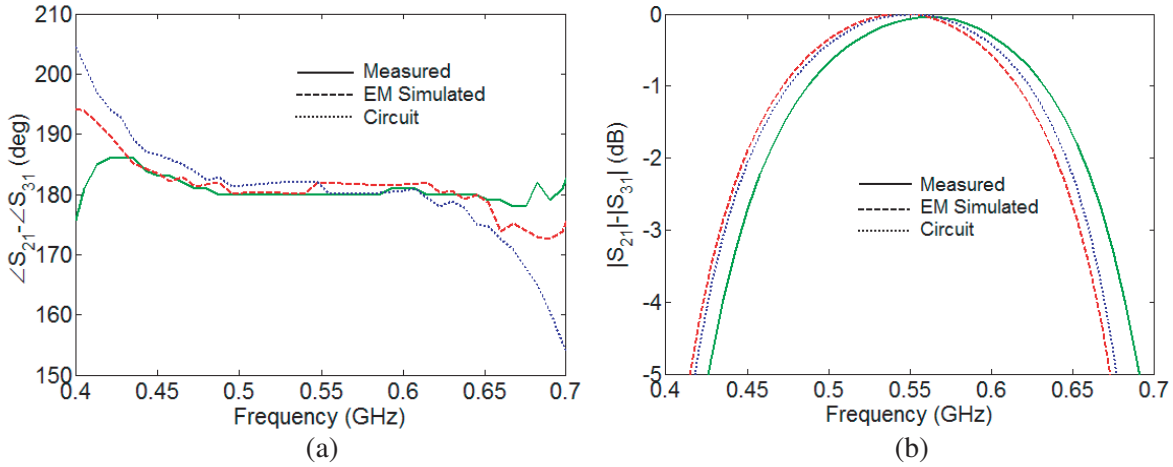

Figure 7. Measured, EM simulated, computed amplitude and phase response of proposed balun. (a) Phase balance. (b) Amplitude balance.

Table 3. Comparison of proposed balun performance with the best reported baluns.

Param. \ Ref.	**Conventional (Ideal)**	**[9]-T**	**[9]-Π**	**[10]**	**[11]**	**Present**
Operating freq., f_0 (GHz)	-	1.0	1.0	1.0	2.4	0.5
Insertion loss at f_0						
$\|S_{21}\|$ (dB)	3.0	3.5	3.6	3.56	2.90	3.64
$\|S_{31}\|$ (dB)	3.0	3.7	3.8	3.5	3.83	3.60
Magnitude Bal. at f_0 $(\|S_{21}\| - \|S_{31}\|)$ (dB)	0.0	0.2	0.2	0.06	0.93	0.04
Phase diff. at f_0 $(\angle S_{21} - \angle S_{31})$ (deg.)	180	NA	NA	177.3	178.63	179.8
FBWs (%) RL (15 dB)	80	73.1	63	70	42	73.8
Magnitude bal. $(0 \pm 1\,\text{dB})$	28	22.8	22.1	25	33	25.5
Phase bal. $(180^\circ \pm 10^\circ)$	44	46.5	52.7	51	33	56.9
Size of balun (λ_g^2)	0.125	0.045	0.031	0.031	0.069	0.033
Occupying Area (%) Relative to conventional design	100	36	25	25	55.8	26
Harmonic suppression up to	No	$4.5f_0$	$4.5f_0$	$6f_0$	NA	$12f_0$

which is about $12f_0$, where a deep suppression is observed from fourth to eighth harmonics, while the overall suppression is better than at least 10 dB. Table 3 compares the performance of the proposed balun with those of best reported balun designs. The proposed balun exhibits excellent magnitude and phase differences at f_0, while various FBWs are better than [9–11]. Besides, the proposed balun has high degree of harmonic suppression up to $12f_0$ which is double of [10], while maintaining the compact area the same as those in [9, 10] with improved bandwidths.

4. CONCLUSION

A design of a multiple (three) stub based compact wide range harmonic suppressed balun is presented. In contrast to other methods that achieve size reduction at the cost of unexpected bandwidth reduction, here, the various bandwidths are predetermined for various levels of size and harmonic reduction. It is shown that the balun using three stub unit exhibits improved bandwidths that are close to those of a conventional balun. Further, a high degree of miniaturization (up to 75%) and spurious suppression (up to twelfth harmonic) is achieved within the realizable impedance values. The proposed balun, based on transmission line analysis, is simple and straightforward with predicted bandwidths, easy to fabricate as no tedious coupled lines and ground plane structures are involved.

REFERENCES

1. Sturdivant, R., "Balun designs for wireless, mixers, amplifiers and antennas," *Applied Microwave & Wireless*, Vol. 5, No. 3, 34–44, 1993.
2. Lin, C. H., C. H. Wu, G. T. Zhou, and T. G. Ma, 'General compensation method for a Marchand balun with an arbitrary connecting segment between the balance ports," *IEEE Transactions on Microwave Theory and Techniques*, Vol. 61, No. 8, 2821–2830, 2013.
3. Bemani, M., S. Nikmehr, and H. Takfallah, "Dual-band microstrip-to-coplanar stripline Wilkinson balun using composite right- and left-handed transmission lines and its application in feeding dual-band bow-tie antenna," *IET Microwaves, Antennas & Propagation*, Vol. 8, No. 7, 532–540, 2014.

4. Zhang, H., Y. Peng, and H. Xin, "A tapped stepped-impedance balun with dual-band operations," *IEEE Antennas and Wireless Propagation Letters*, Vol. 7, 119–122, 2008
5. Barik, R. K., K. V. P. Kumar, and S. S. Karthikeyan, "Design of a dual-band microstrip branch-line balun using T-shaped coupled lines," *Wiley Microwave and Optical Technology Letters*, Vol. 59, No. 5, May 2017.
6. Li, J. L. and S. W. Qu, "Miniaturized branch-line balun with bandwidth enhancement," *Electronics Letters*, Vol. 43, No. 17, 931–932, 2007.
7. Kim, P., G. Chaudhary, and Y. Jeong, "Analysis and design of a branch-line balun with high-isolation wideband characteristics," *Wiley Microwave and Optical Technology Letters*, Vol. 57, No. 5, May 2015.
8. Park, M.-J. and B. Lee, "Stubbed branch line balun," *IEEE Microwave Wireless Components Letters*, Vol. 17, 169–171, Mar. 2007.
9. Velidi, V. K., A. Pal, and S. Sanyal, "Harmonics and size reduced microstrip branch line baluns using shunt open stubs," *International Journal of RF and Microwave Computer-Aided Engg.*, Vol. 21, No. 2, 199–205, Mar. 2011.
10. Velidi, V. K. and S. Sanyal, "Wide range suppressed harmonic response compact microstrip balun," *International Journal of Electronics and Communications*, Vol. 66, 45–48, 2012.
11. Kumari, A., P. Bhowmik, and T. Moyra, "Design and validation of miniaturize rat race coupler based microstrip balun," *International Journal of Electronics and Communications*, Aug. 2018, doi: https://doi.org/10.1016/j.aeue.2018.08.013.